BS 2019 2-4 SEPT ROME 16th IBPSA INTERNATIONAL CONFERENCE AND EXHIBITION

INTERNATIONAL BUILDING PERFORMANCE SIMULATION ASSOCIATION

Handling 3D Model for Urban Thermal Study with the Finite Element Method

Nicolas Duport, Jairo Acuña Paz y Miño, Benoit Beckers
Urban Physics Joint Laboratory, Université de Pau et des Pays de l'Adour, E2S UPPA, Anglet, France

Abstract

We are interested in the thermal behaviour of an urban scene. Two techniques are used to characterize this phenomenon: thermography and computational simulation. Their parallel use leads towards a better understanding of the involved physical parameters. First, we present the geometry of the scene and its implementation in the CAST3M finite element software (El Ganaoui, 2005), developed by the CEA (French Alternative Energies and Atomic Energy Commission). Then, we present a development to highlight the influences of thermography on the assumptions of numerical simulation. The results allow evaluating the physical material parameters meaning, particularly, the radiant specular component of the windows.

Introduction

The energy balance of a building, even analysed independently, strongly depends on the physical configuration of the more or less close neighbourhood. For estimating energy consumption on an urban scale, the building by building balance becomes difficult if not impossible (Pignolet-Tardan, 1997). Therefore, urban energy consumption has been a critical research subject for the last 30 years (Keirstead et al, 2012) and it will certainly still remain a major concern in the near future.

Different approaches and models have been developed in order to simulate building heating and cooling power demand, from the building scale to the urban scale including the district scale. Among them, the models based on nodal method (Bouyer, 2011) are often used, mainly because they are relatively cost effective compared to other more detailed models. However, this time saving is at the price a too simple geometric information (Frayssinet 2018).

The finite element method (FEM) was initially developed in mechanics and civil engineering (structural design) in the last third of the 20th century (Zienckiewicz, 1967). The FEM has the advantage of taking into consideration the actual geometry of the project according to the spatial distribution of the elements, and it allows different visualizations of results.

However, until now, applications related to thermal phenomena (Lewis, 2004) remain little used for building thermal design.

There are many experimental methods that allow qualifying the thermal behaviour of a room, a building or more generally an urban scene. Among them, infrared thermography (IRT) is a diagnostic tool for detecting disorders that may be invisible to the naked eye (Kirimtat, 2018). It allows, with one image, to detect local thermal variations, and therefore to visualize insulation anomalies, or to confirm suspected defects without affecting the object of study, as IRT is a non-destructive technique (S.S. de Freitas, 2014). In short, thermography makes it possible to collect big amounts of data on a single capture without losing the spatialized information. This aspect makes it useful for calibrating numerical simulations (Evangelisti, 2018, Lalanne 2015).

Recently, some contributions were concerned in simulating thermograms at an urban scale, with simplified geometric models (Ghandehari 2018, Kubilay 2018, Aguerre 2019). The objective of this paper is to manage a model of a street with a high level of detail, in order to perform a simulation on its thermal behaviour, with the finite element method.

Methodology

To carry out a suitable study with the finite element method, it is necessary to implement a congruent and not too distorted mesh. The method used to build this mesh is to create a structured geometric model in a CAD software, and to directly introduce it as input data into a finite element software. Therefore, the geometric model is the mesh of the simulation. In order to facilitate the calculation and the interpretation of the results, we put some restrictions on the physical model a cloudy winter day is chosen where most of the information deals with the conduction and convection phenomena. The test case concerns a historical street, representative of the city of Bayonne, with a non-homogeneous composition of facades and a complex geometry.

Geometric model description

Modelling urban scenes is a task in which complex man-made environments have to be represented accurately. The lack of information needed for the construction of an urban model is one of the main difficulties, especially in dense urban environments (Beckers, 2010).

This study is based on a CAD congruent geometric model of the rue des Tonneliers, which is located in the city centre of Bayonne (France, 43.48° N) (Acuña, 2018). The model is composed of about thirty buildings oriented North-South, Figure 1. The street is about one-hundred-meter-long and five meter wide. Buildings comprise between three and five levels for an average height of 14m. The walls and floors are all 0.15m thick.

https://doi.org/10.26868/25222708.2019.210563

a)Aerial view of the Tonneliers street.

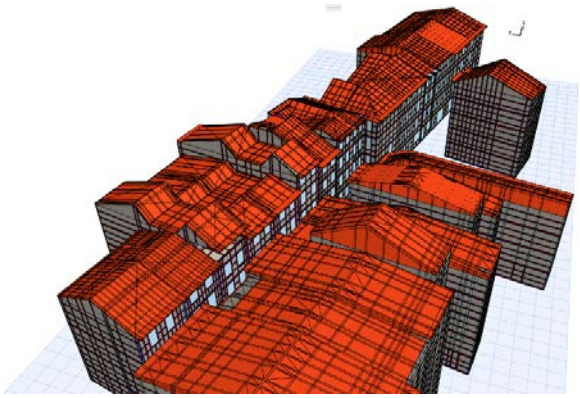

b) CAD model of Tonneliers street.

c)Inside view of the street.

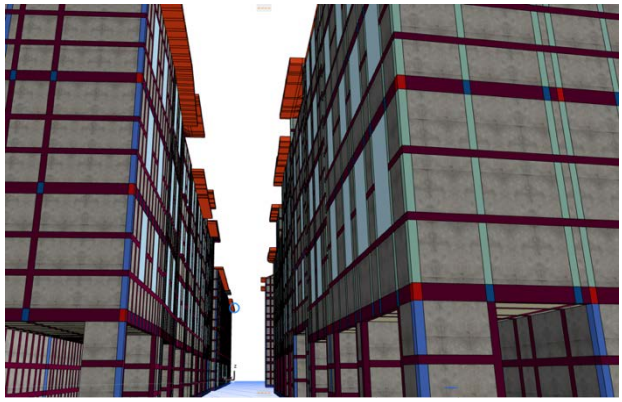

d)Inside view of the modelled street.

Figure 1: Modelling the Tonneliers street.

This street is located at one of the densest districts in France and it offers the possibility to model a geometry with a satisfactory level of details. Indeed, the multi-material façades of this district date mainly from the 18th and 19th centuries and feature simple half-timbered walls.

This constructive system had the advantage of allowing overlapping corbelled floors, in order to leave a wide enough passage on the public road and to save space in the upper floors. The architecture of Bayonne is essentially characterized by the narrowness of the streets. Eaves and mullioned windows are also very common and as it will be shown later, they have a significant impact on the thermal behaviour of buildings.

Particular attention is paid to the type of mesh used (only hexahedrons and prisms) as this will impact on the quality and accuracy of the FEM calculation as well as on its further interpretation (Blocken, 2015). Regarding the architectural style of the model, hexahedrons make it possible to faithfully reproduce the geometry. They allow a more visual representation of the results and they are less time consuming to compute; being the number of nodes is lower than with a tetrahedral mesh. Prisms are exclusively present to match the steep character of the roofs.

In the present case, the CAD mesh is directly used as a finite element mesh. The data is exported from the CAD software using an OBJ file. This is a geometry definition file format first developed by Wavefront Technologies. OBJ files can contain scale information in a human readable comment line. This has a huge advantage regarding the high number of elements of the model.

Then, a python script allows to transform the information needs from the OBJ into Gibiane, which is the language used by Castem: a first list containing all the points of the project and a second one containing the volume elements are produced. Each element is described according to its faces and these faces refer to the points contained in the first list. The volume elements make possible to materialize the phenomenon of thermal conduction while thermal convection must be applied to surfaces. It is therefore necessary to automatically identify the internal and external cavities of each building in order to assign the values of convection coefficients and to ensure accurate boundary conditions. From the list of elements, it is easy to define their faces. If a face is present twice, it is an inner face linking two elements. If a face only appears once, it belongs to the skin of the volume. It is then necessary to differentiate between the faces belonging to the inner skin and those belonging to the outer skin. The physical parameters of the different materials are applied according to the colour code used in the CAD software.

The entire model brings a total of 124311 volume elements 99% being hexahedrons. The interior envelope is composed by 137390 quadrilaterals and the exterior envelope by 87894.

For simplicity's sake, the different buildings composing the street are built independently and are then assembled together to form the street. As a result, there is no "link" between the buildings to represent the thermal conduction phenomenon between the dwellings. This connection is made inside the calculation software. Precisely, any point in the slave mesh is given by a combination of the node temperatures of the master mesh in which it is located, Figure 2. This combination is related to the shape functions N(x) describing the mesh element:

$$T(M) = N(x_M).T_I + N(x_M).T_J + \mathrm{N}(x_M).T_K + N(x_M).T_L \quad (1)$$

where x_M is the coordinates of the point M in the local basis of master element.

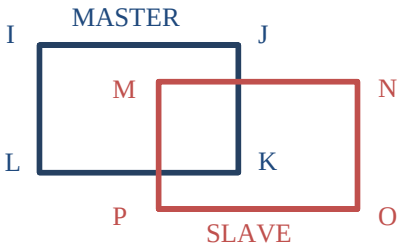

Figure 2: Nodes connexions between buildings

Equation (1) can be written as follow:

$$T(M) - (N(x_M).T_i + N(x_M).T_j + \mathrm{N}(x_M).T_K + N(x_M).T_L) = 0 \quad (2)$$

This relation is imposed using lagrangian multipliers and it represents the mutual interaction between the two surfaces (Charras, 1993).

Physical base

Carrying out a thermal study during the winter period makes it possible to highlight the different conductivities of buildings. Under these conditions, it is possible to observe the behaviour of users inside the dwellings from the exterior. The high level of details of the model allows seeing the thermal behaviour of the different materials. The simulations and measurements took place during the late afternoon, under a cloudy sky and in steady state.

Beckers (2013) assumes that the flux between two infinite walls at temperatures differing from one degree, is reaching 6 W.m^{-2} at 297 K according to the Stefan-Boltzmann law. In our case, due to the lack of shortwave, we can fairly think that the difference of temperature between two surfaces facing each other is not high enough to have a significant influence.

We start with the classical equation of heat conduction in a solid:

$$div[k\ grad\ T] + Q = \gamma c \frac{\partial T}{\partial t} \quad (3)$$

where T is the temperature in Kelvin, k is the thermal conductivity in W.m^{-1}K^{-1}, t is the time, γ is the density in kg.m^{-3}, Q is the heat density in W.m^{-3} and c is the specific heat capacity in J.kg^{-1}. K^{-1}. Fourier's law provides the variable conjugated to the temperature: the heat flux $\vec{q}$, (W.m^{-2}):

$$\vec{q} = -k\ \overrightarrow{grad}\ T \quad (4)$$

The FEM allows to reach efficiently an approached solution (Zienckiewicz, 1967). The purpose of this method is to determine a function that is a solution of the partial differential equation for given boundary conditions. The EDP describes the physical phenomenon of the system (i.e. Fourier's law for thermal conduction or laws of elasticity for material strength) and the boundary conditions are restraining the system. The later consist of Dirichlet, where the temperature is imposed. Neumann conditions where the heat flux is imposed.

Let us consider the steady state equation:

$$\frac{\partial}{\partial x}\left(k_x \frac{\partial T}{\partial x}\right) + \frac{\partial}{\partial y}\left(k_y \frac{\partial T}{\partial y}\right) + \frac{\partial}{\partial z}\left(k_z \frac{\partial T}{\partial z}\right) + Q = 0 \quad (5)$$

Each element exchanges energy with another element through the shared face. Also, each element can deal with a face *S1* subjected to convection and/or another one *S2* loaded with a heat flux. The above differential equation with its boundary conditions correspond to the variational integral below:

$$I(T) = \frac{1}{2}\int_\Omega \left[k_x\left(\frac{\partial T}{\partial x}\right)^2 + k_y\left(\frac{\partial T}{\partial y}\right)^2 + k_z\left(\frac{\partial T}{\partial z}\right)^2 - 2QT\right] d\Omega + \int_{S2} qT dS + \frac{1}{2}\int_{S1} h(T - Ta)^2 dS \quad (6)$$

The domain Ω is divided into n number of finite elements and each element has r nodes. The temperature is expressed in each element:

$$T_e = [N]\{T\} \quad (7)$$

with the shape function matrix $[N]$ and $[T]$ the vector of nodal temperatures:

$$[N] = [N_i, N_j, \dots, N_r]$$

$$\{T\} = \begin{Bmatrix} T_i \\ \dots \\ T_r \end{Bmatrix}$$

When there is no heat generation within the model (Q=0), the second term of the first integral of $I(T)$ disappears. Similarly, if an insulated boundary is present, the second integral and/or the last integral is eliminated. Finally, considering the entire scheme, Lewis (2004) assumes that the above equation can be written in a compact form:

$$[K]\{T\} = \{f\} \quad (8)$$

$$[K] = \int_\Omega [B]^T[D][B]d\Omega + \int_S h[N]^T[N]dS$$

$$\{f\} = \int_S hT_a[N]^T dS - \int_P q[N]^T dS$$

with:

$$[B] = \nabla[N]^T$$

$$[D] = \begin{bmatrix} k_x & 0 & 0 \\ 0 & k_y & 0 \\ 0 & 0 & k_z \end{bmatrix}$$

The resolution of this system of linear algebraic equations enables to obtain the unknown temperatures at each node. A graphic representation of the temperatures of nodes on the model surface constitutes the basis to see the behaviour of the scene.

Test case description

The experimental work consisted of a sequence of photographs and thermograms (longwave) taken at 18:00

p.m on December 9th, 2018, under a cloudy sky with no wind. The main goal of this measurement campaign was to detect conductivities and/or defects of the different façades. Infrared images were taken with the FLIR T460 camera. The camera lens has an aperture of 90° in the horizontal plane and 73° in the vertical plane. The distance between the camera and the object was set to 0m and the emissivity was set to 1 in order to eliminate the influence of the surroundings and to cancel the thermal effect of the ambient layer between the scene and the camera (Kylili, 2014). The observed apparent temperatures were deduced from the total radiant power emitted in the spectral range that reached the lens of the camera (7.5-13 μm).

The environmental and boundary conditions were obtained whenever possible from the on-site measurements or estimated. The outside air temperature (12°C) was measured on-site at the time the images were taken. The inside air temperature was fixed to 18°C for the first simulation and evolves with the different simulations. Outside, convection coefficients depend on many parameters but strongly on the speed and direction of the wind (Mirsadeghi, 2013). The wind velocity was very low on the selected day. Therefore, the outside coefficient was fixed to 10 $W.m^{-2}.K^{-1}$ in agreement to the models available in the literature. Regarding the inside convection coefficients, the French thermal regulation specifies the value: 2.5 $W.m^{-2}.K^{-1}$ for the inside cavities and 5 $W.m^{-2}.K^{-1}$ for the roof.

a) Photograph of the street.

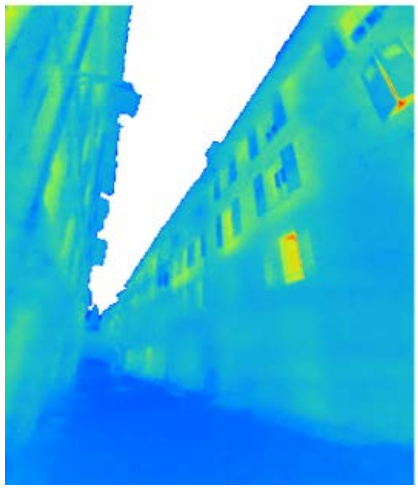

b) Infrared thermogram of the street.

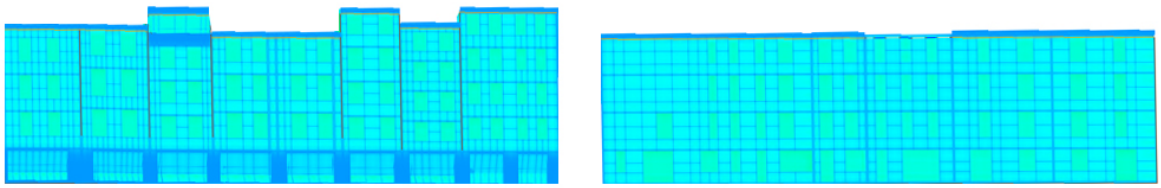

c)Simulated south side of the street.

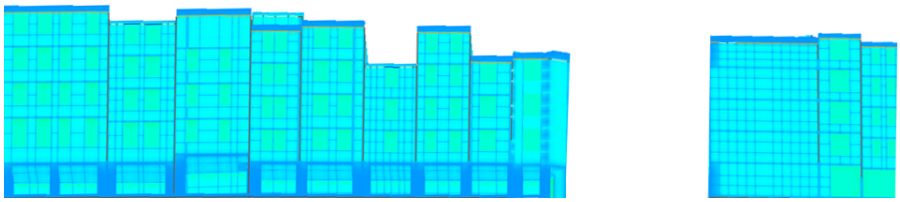

d) Simulated north side of the street.

Figure 3: Overall street simulation.

Tonnelier's street surfaces display a rich heterogeneity of materials. The level of detail of the present case model allows a simulation with four materials: roof, wood, cob and windows. Thermal properties were described using the thermal conductivity, k ($W.m^{-1}K^{-1}$):

- Roof: 0.5 $W.m^{-1}K^{-1}$
- Window: 2 $W.m^{-1}K^{-1}$
- Wood: 0.2 $W.m^{-1}K^{-1}$
- Cob: 1 $W.m^{-1}K^{-1}$

The material properties have been defined from both experimental data collection and assumptions based on *in situ* observations.

Results and discussions

A first simulation was carried out with assumptions specific to the period of year. Precisely, we assumed that all the inhabitants heat to an average temperature of 18°C, the first extreme cold has not yet arrived. All the dwellings have the same wall compositions, with simple glazing and no insulation, Figure 3. The ground as well as the sky vault have not been modelled because in this study, we limit ourselves to a convection conduction system.

As expected, we can notice on the thermogram that the surface temperatures of the different buildings are homogeneous. However, it appears stains with a higher temperature corresponding to the windows. Since the thermal conductivity of windows is higher than other materials used in the façade, it is more likely to conduct heat. The window in the middle of the photo, which has a much higher temperature than the others, corresponds to a window opened when the thermography was taken (we can see it on the visual photo).

On simulated thermography, we find the same orders of magnitude for apparent surface temperatures. We observe the grid marked by the different materials that make up the model. The eaves are colder on the simulation than on the measured thermography. In reality, these elements are cooled in the upper part by radiation from the sky vault and heated in the lower part by radiation from the building facades. However, in our simulated model, radiation not being taken into account, these elements are only subjected to heat exchanges by convection with the outside air of the street.

This first simulation allows us to lay the foundations of our method. It shows that it is possible to carry out a simplified thermal study on an urban model with a high level of detail by linking CAD model and finite element mesh. The solutions were obtained after different simulations, each taking about one minute. The calculation times being rather short, most of this step was to obtain the geometry of the model.

To go further in the thermal analysis of the street, infrared photos were taken in order to highlight anomalies or differences between dwellings. On the thermography, Figure 4, we immediately notice hotter stains corresponding to apparent temperature differences. Some of them correspond to dwellings where it can be assumed that inhabitants have turned on their heating. Moreover, there is a little hot surface under the left window of the third floor of the left building. Looking at some of the dwellings on this street, we realized that this detail could correspond to a radiator on. Indeed, it is often accepted that in these dwellings, heat sources were positioned under windows in order to warm living rooms. To simulate this phenomenon, the temperature of part of the mesh forming the inner wall below the window is set at a high temperature.

The first two floors of the left and central buildings have the same apparent surface temperatures. For the simulation, we assumed that these floors are unoccupied and therefore have a lower interior temperature than the others. Below these two apartments, the hot lines correspond to electrical lines that emit heat by Joule effect. Simulated thermography has the same orders of magnitude as infrared images. We can see the three apartments that have a higher apparent surface temperature. The two unoccupied apartments have a colder one. If the temperature difference between exterior and interior is not significant enough, there is an apparent temperature homogeneity on the materials that make up the façade. This is the case for the first apartment in the central building, for which no difference between the lime mortar and the half-timbered wood is visible.

Concerning joinery, several cases can be studied. Firstly, the window shutters are error-prone because they are not present in the simulated model. In order to interpret their thermal behaviour, time plays a major role. If the shutters are open and have been closed recently before the picture is taken, they will be at air temperature. If the latter have been closed for a while, then they will appear with a warmer temperature because they are heated by the windows. Secondly, the windows themselves must be broken down into two parts: the wooden joining elements and the glass. We focused here on glass, which offers a greater apparent temperature difference depending on several parameters. On the visual photo of the buildings, we can easily see that the glass in the windows behaves like a mirror. i.e. it reflects the elements in the direction of the angle of incidence from which the camera is directed. Thus, the windows on the third floor of the central building reflect the cloudy sky (light grey) while the windows on the top floor of the right building reflect the eave projection. We find the same phenomenon on images characterizing long waves. This is due to the fact that the specular part of the waves reflected by the glass is larger than for the other materials composing the façade. Another example is shown in the right-hand window on the second floor of the central building. On the visual photograph, we can clearly see a light part corresponding to the cloud cover and a darker part corresponding to the roof of the building on the other side of the street. In the same way as before, we find the same phenomenon on the infrared photo.

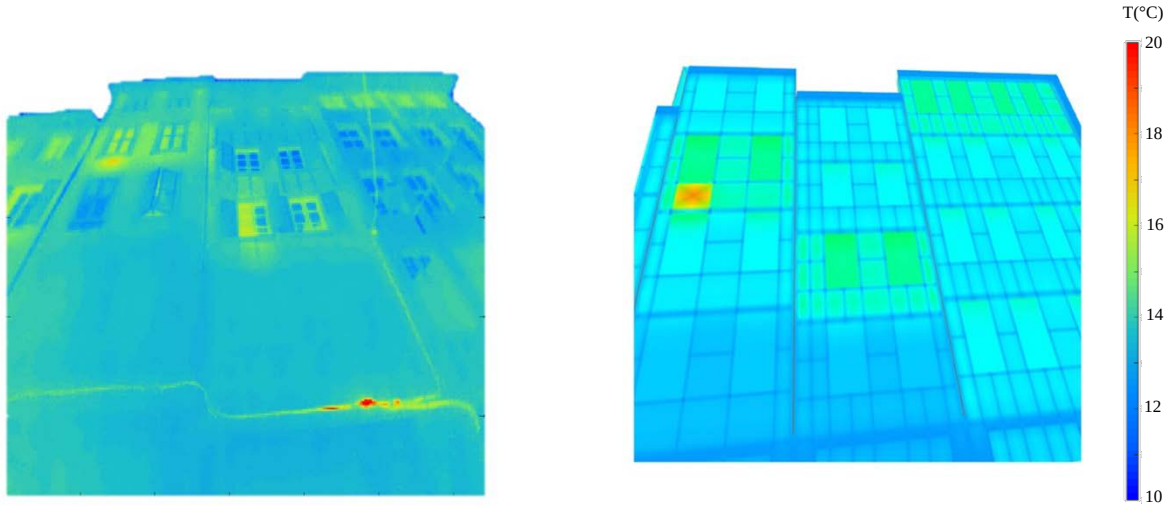

a) Measured thermogram. *b) Simulated thermogram.*

c) Photograph of buildings.

Figure 4: Highlight the specular component of the infrared reflexion of the windows.

In most simulations of thermal radiation, it is assumed that all materials in the building domain are assumed to be black bodies with completely diffuse emission. This is not the case for glass in carpentry. This phenomenon is not found in the present simulation because long wave radiation was not taken into account in our study. Finally, the camera's point of view is very important for the interpretation and understanding of the thermal behaviour of windows.

On the second case study, Figure 5, we find the same phenomenon as presented above concerning windows. We see clearly the specular reflections of glass. For the thermography simulation, we assumed an indoor air temperature of 18°C in all apartments with insulation (thermal conductivity equal to 0.05 $W.m^{-1}. K^{-1}$). The last apartment in the central building was modelled with an indoor temperature of 22°C and the apartment below had no insulation and kept the same physical parameters as in the previous simulations.

Our analysis focuses on the building in the centre of the photo. If we focus on the Figure 5 b), we can detect the apartment that does not have insulation. This results in a warmer surface temperature than the rest of the façade and allows us to see the half-timbering. The first two apartments have a rather homogeneous façade temperature. A lack of heating inside the apartment could have been chosen as a hypothesis, but the presence of hot carpentry led to the choice of simulating heating with insulation in the façade. The difference in the appearance of the joineries comes from the presence or not of the shutters.

Furthermore, putting more intense heating inside the last apartment induces a higher surface temperature on the simulated thermography (joinery and facings). The warmer temperature aspect of the joinery may not only be due to the more intense heating but also to the specular reflection perceived by the camera due to eaves. There is an apparent temperature difference on the façade of the last apartment between simulated and measured

thermography. On the last one, we can see a colder apparent temperature than on the first one. Two possibilities can explain this phenomenon: more insulation on this dwelling or a refreshment due to the long wave radiation of the sky vault. If this second explanation was the right one, the apartments in the next building (Figure 5, a)) would also be colder than the others. However, we can see that this is not the case, so this possibility can be discarded. More generally, there is a slight gradation in temperature from the ground to the roofs. The surface with lower surface temperatures were those with a higher sky view factor. Indeed, the closer a surface is to the roof, the greater its view of the sky factor is and the more energy that surface will exchange with the sky vault. However, since the radiative balance of a surface in our model is negative, it cools as its sky view factor increases. As before, this phenomenon is not found in simulated thermography because long wave radiation has not been taken into account.

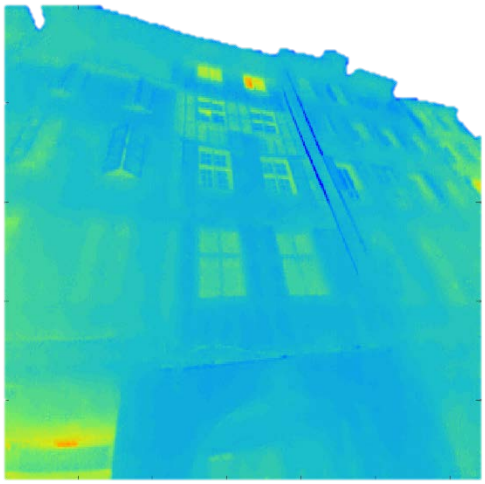

a) Measured thermogram.

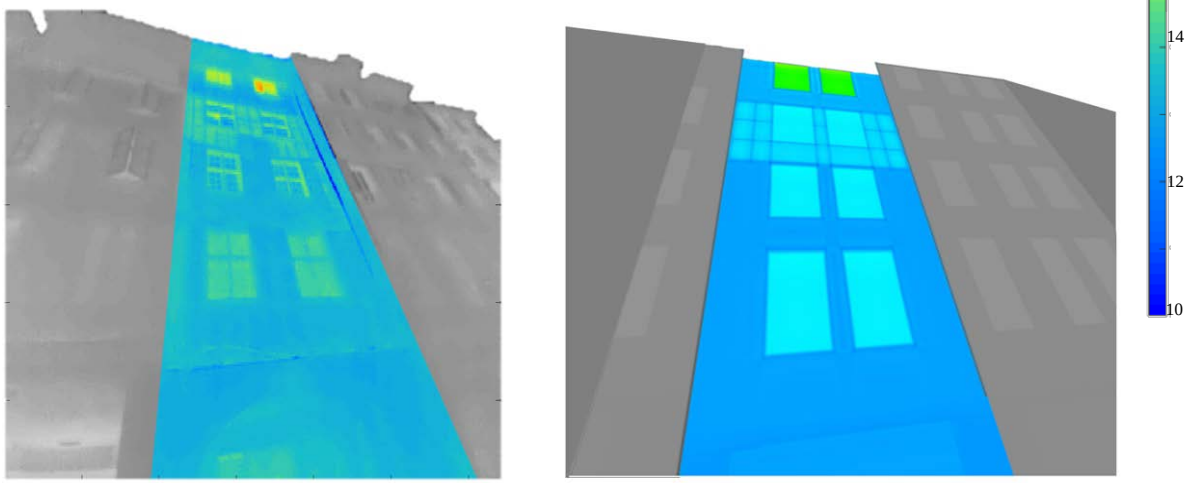

b) Comparison between measured and simulated thermograms of the central building.

Figure 5: Building with isolated dwellings and a non-insulated.

A comparison of temperatures on specific points belonging to the facades of street buildings would not be appropriate in our case because predominant parameters were deliberately omitted in this study. Nevertheless, the orders of magnitude remain acceptable and the method presented makes it possible to obtain an additional tool for a more global and precise understanding of the physical phenomena involved within an urban site.

In future simulations, considering the entire problem would allow validating the hypotheses concerning the physical parameters of the materials but also on the usages. The radiation phenomenon will involve storing the form factors matrix and the size of this matrix can reach the limitation of the Cast3m framework.

Conclusion

The work presented in this paper has shown that it is possible to simulate thermograms on a geometric model of an urban site with a high level of detail. In the presented example, the level of detail is sufficient to perceive the thermal behaviour of the buildings composing the street.

The comparison between measured and simulated thermograms allows to confirm that the conduction-convection system is predominant during a cloudy winter day. The experimental spatialized method brings additional information that can be used as a simulation parameter (heating, insulation). In the same way, the simulation provides answers to questions arising from the interpretation of thermograms, for example the radiant specular component of the windows that appear in the measurement and not in the simulation.

References

Acuña Paz y Miño, J., Lefort, V., Lawrence, C. and Beckers, B. (2018). Maquette Numérique d'une rue du vieux Bayonne pour son étude thermique par éléments finis. *A la pointe du BIM, Ingénierie & architecture, enseignement & recherche* (ed. Eyrolles) 103–115, Clermont-Ferrand (France), May 15-16 2018.

Aguerre, J. Nahon, R. Garcia Nevado, E. La Borderie, C. Fernández, E. and Beckers, B. (2019). A street in perspective: Thermography simulated by the finite element method. *Building and Environment*, *Volume 148*.15 January 2019. 225-239.

Beckers, B., Rodriguez, D., Antaluca, E. and Batoz, J.L. (2010). About solar energy simulation in the urban framework: the model of Compiègne. *3rd International Congress Bauhaus SOLAR. November 10-11 2010, Erfurt, Germany*.

Beckers, B. (2013). Taking Advantage of Low Radiative Coupling in 3D Urban Models. *Eurographics Workshop on Urban Data Modelling and Visualisation*. May 6-10-2013, Girona (Spain).

Bouyer, J., Inard, C., Musy, M. (2011). Microclimatic coupling as a solution to improve building energy simulation in an urban context. *Energy and Building*. 43(7) pp.1549-1559.

Blocken B. (2015). Computational Fluid Dynamics for urban physics: Importance, scales, possibilities, limitations and ten tips and tricks towards accurate and reliable simulations. *Building and Environment 91*. 219–245.

Charras, TH., Millard, A. and Verpeaux, P. (1993). Solution of 2D and 3D contact problems by means of Lagrange multipliers in the castem 2000 finite element program. *Transactions on Engineering Sciences. Vol 1. WIT Press, ISSN.*

De Freitas, S.S., and De Freitas V.P. and Barreira, E. (2014). Detection of façade plaster detachments using infrared thermography - a nondestructive technique. *Construction and Building Materials. Volume 70*. 80–87.

El Ganaoui, K. and Allaire, G. (2005). Homogenization of a conductive and radiative heat transfer problem, simulation with Cast3m. *Proceedings of HT2005, 2005 ASME Summer Heat Transfer Conference*. July 17-22, 2005. San Francisco, California, USA.Evangelisti, L., Guattari, C., Gori, P. and Asdrubali, F. (2018). Assessment of equivalent thermal properties of multilayer building walls coupling simulations and experimental measurements, *Building and Environ*ment. Volume *127*. 77–85.

Frayssinet, L. Merlier, L., Kuznik, F., Hubert, J.L., Milliez, M., Roux, J.J. (2018). Modeling the heating and cooling energy demand of urban buildings at city scale. *Renewable and Sustainable Energy Reviews*. Vol 81, Part 2, Pages 2318-2327.

Ghandehari, M., Emig, T. and Aghamohamadnia, M. (2018). Surface temperatures in New York City: geospatial data enables the accurate prediction of radiative heat transfer, *Scientific Reports*. 8 (1). 1–10.

Keirstead, M. Jennings, Sivakumar, A. (2012). A review of urban energy system models: approaches, challenges and opportunities. *Renewable and Sustainable Energy Reviews*, 16(6) pp.3847-3866.

Kirimtat, A. and Krejcar, O. (2018). A review of infrared thermography for the investigation of building envelopes: advances and prospects, *Energy and Building*. *176*. 390–406.

Kylili, A., Fokaides, P.A., Christou, P. and Kalogirou, S.A. (2014). Infrared thermography (IRT) applications for building diagnostics: a review. *Applied Energy 134*. 531–549

Kubilay, A., Derome, D., Carmeliet, J. (2018). Coupling of physical phenomena in urban microclimate : A model integrating air flow, wind-driven rain, radiation and transport in building materials. *Urban Climate*. Vol 24, pp 398-418.

Lalanne, N., Krapez, J.C., Le Niliot, C., Briottet, X., Pierro, J. and Labarre, L. (2015). Development and validation of a numerical tool for simulating the surface temperature field and the infrared radiance rendering in an urban scene. *Quantitative InfraRed Thermography. J. 12 (2)*. 196–218.

Lewis, R.W., Nithiarasu, P. and Seetharamu, K.N. (2004). Fundamentals of the Finite Element Method for Heat and Fluid Flow. *John Wiley & Sons*.

Mirsadeghi, M., Cóstola, D., Blocken, B. and Hensen. J.L. (2013). Review of external convective heat transfer coefficient models in building energy simulation programs: implementation and uncertainty. *Applied Thermal Engineering. 56 (1–2).* 134–151

Pignolet-Tardan, F., Depecker, P. and Gatina, J-C. (1997). Modélisation du comportement thermique d'un espace urbain : Calcul de la réponse en température des structures et de l'air ambiant. *Revue générale de thermique, Volume 36, Issue 7*, July-August 1997. 534-546.

Zienkiewicz, O.C., (1967). The Finite Element Method in Structural and Continuum Mechanics, McGraw-Hill pp.